HEFAT 2005
4 th International Conference on heat Transfer, Fluid Mechanics and Thermodynamics
19-22 September 2005, Cairo, Egypt
SS3

NUMERICAL STUDY OF THE EVAPORATION OF A FALLING OSTWALDIAN FILM ALONG AN INCLINED FLAT PLATE INTO A LAMINAR STREAM OF HUMID AIR

S. SAOULI [1*], M. BOUMAZA [2] , N. SETTOU [1] , S. AIBOUD-SAOULI [3] and M. DAGUENET [4]

[1] Faculté des Sciences et Sciences de l'ingénieur, Université de Ouargla, Route de Ghardaïa, Ouargla 30000, Algérie
E-mail : sveralgk@yahoo.fr
***** Author responsible for the correspondance
[2] Institut de Génie Climatique, Faculté des Sciences de l'ingénieur, Université de Mentouri, Route de Ain-El Bey, Constantine, 25000, Algérie
[3] Institut de Formation Professionnelle, Said Otba, Ouargla, 30 000, Algérie
[4] Laboratoire de Thermodynamique et Énergétique, Université de Perpignan, 52 Avenue de Villeneuve, 66800 Perpignan Cedex, France

ABSTRACT
The present paper deals with the evaporation of a falling Ostwaldian film along an inclined isothermal plate into a laminar stream of humid air. The governing boundary-layer and the matching conditions are solved using a finite-difference method. Four liquids are considered : two pseudoplastic, and the other two dilatant. The effect of the air flow conditions, the
inclination and the temperature of the plate, as well as the inlet temperature of the film on the evaporation rate and the thickness were studied. A comparative analysis between one dimensional, partial two-dimensional and full two-dimensional approches is made. It was found that the inertia terms cannot be neglected in the momentum equation of the liquid film, and these differences increase as the flow behaviour index increases.

NOMENCLATURE
D_V	mass diffusivity (m^2/ s)
g	gravitational acceleration (m/ s^2)
h	latent heat of vaporization (J/ kg)
K	liquid consistency index (Pa s^n)
L	plate length (m)
$\dot{m}_I$	interfacial mass flux (kg/ m^2 s)
Mr	dimensionless evaporation rate
M_a	molar mass of air (kg/ Kmol)
M_v	molar mass of vapor (kg/ Kmol)
n	flow behaviour index of the liquid
P	pressure (Pa)
Q_0	inlet liquid mass flow rate (kg/ m s)
T	temperature (K)
T^*	dimensionless temperature
U,V	axial and transverse velocities (m/ s)
U^*	dimensionless axial velocity
W	mass fraction of water vapor
W^*	dimensionless mass fraction of water vapor
x,y	coordinates in the flow and transverse directions (m)
X^*	dimensionless coordinate in the flow direction

Greek symbols

α	thermal diffusivity (m^2/ s)
δ	local liquid film thickness (m)
δ^*	dimensionless liquid film thickness
ΔX^*	grid size in the flow direction
$\Delta\eta$	grid size in the transverse direction
λ	thermal conductivity (W/ m K)
μ	dynamic viscosity (N s/ m)
ν	kinematic viscosity (m^2/ s)
θ	inclination angle of the plate (rad)
ρ	density (kg/ m^3)
τ	shear stress (Pa)

Subscripts

G	mixture (air+water vapor)
I	condition at the liquid-gas interface
L	liquid
P	plate
0	inlet
∞	free stream

INTRODUCTION
Gas-liquid flow with coupled heat and mass transfer is widely encountered in many industrial processes. Some prominant examples include cooling towers, evaporators, turbine blade cooling, and drying. Because of its widespread practical application, liquid film evaporation and related heat and mass transfer phenomena have been extensively studied. Numerical studies of liquid film

cooling or evaporation include evaporation of single or two-component liquid film along a flat plate or a channel in laminar or turbulent forced, natural or mixed convection [1-15].

In these studies, the liquid films are considered to be Newtonian. The case of evaporating non-Newtonian liquid films does not seem to have been treated yet. The objective of the present paper is to investigate the evaporation of a gravity-driven Ostwaldian liquid film into laminar stream of a humid air along an inclined isothermal flat plate.

PHYSIAL MODEL AND GOVERNING EQUATIONS

The geometry of the problem under consideration is shematically represented in Figure 1. An isothermal plate with inclined angle θ is maintained at temperature T_P and wetted by a gravity-driven Ostwaldian thin film fed at the plate temperature and with an inlet film thickness of δ_{L0}. The film flows laminarly along the plate in the presence of a parallel downstream laminar gas flow at free-stream velocicy U_∞, ambient temperature T_∞ and mass fraction of water vapor W_∞. As heat is transferred from the plate to the gas stream across the liquid film, simultaneous mass transfer to the gas flow occurs at the interface while the liquid is evaporating.

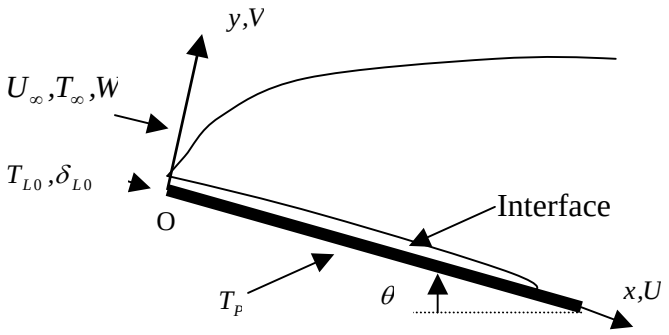

Figure 1: Schematic diagram of the physical system.

The falling liquid film is a non-Newtonian fluid obeying the standard power-law viscosity model :

$$\tau = K\left|\frac{\partial U_L}{\partial y}\right|^{n-1}\frac{\partial U_L}{\partial y} \tag{1}$$

The process is modeled with the following assumptions :

(1) The thermophysical properties of the liquid film and air-vapor mixture are constant.
(2) The boundary-layer assumptions are valid in the liquid as well as in the gas.
(3) The radiative heat transfer, viscous dissipation, surface tension, Soret and Dufour effects are neglected.
(4) The liquid-gas interface is at thermodynamic equilibrium and waveless.
(5) The liquid and gas flows are considered two-dimensional, steady, incompressible and laminar.

Under these assumptions the boundary-layer governing equations are[16]:

2.1. *Liquid phase flow*

$$\frac{\partial U_L}{\partial x}+\frac{\partial V_L}{\partial y}=0 \tag{2}$$

$$U_L\frac{\partial U_L}{\partial x}+V_L\frac{\partial U_L}{\partial y}=g\sin\theta+\frac{nK}{\rho_L}\left|\frac{\partial U_L}{\partial y}\right|^{n-1}\frac{\partial^2 U_L}{\partial y^2} \tag{3}$$

$$U_L\frac{\partial T_L}{\partial x}+V_L\frac{\partial T_L}{\partial y}=\alpha_L\frac{\partial^2 T_L}{\partial y^2} \tag{4}$$

In the one-dimensional approach, the left hand side of eq (3) and (4) are ignored, while in the partial two-dimensional approach, the left hand side of eq (3) and the second term of the left hand side of eq (4) are canceled.

2.2. *Gas phase stream*

$$\frac{\partial U_G}{\partial x}+\frac{\partial V_G}{\partial y}=0 \tag{5}$$

$$U_G\frac{\partial U_G}{\partial x}+V_G\frac{\partial U_G}{\partial y}=\nu_G\frac{\partial^2 U_G}{\partial y^2} \tag{6}$$

$$U_G\frac{\partial T_G}{\partial x}+V_G\frac{\partial T_G}{\partial y}=\alpha_G\frac{\partial^2 T_G}{\partial y^2} \tag{7}$$

$$U_G\frac{\partial W}{\partial x}+V_G\frac{\partial W}{\partial y}=D_V\frac{\partial^2 W}{\partial y^2} \tag{8}$$

2.3. *Boundary and interfacial matching conditions*

$$x=0$$
$$U_L=U_{L0}(y),T_L=T_{L0},U_G=U_\infty,T_G=T_\infty,W=W_\infty \tag{9}$$

$$y=0$$
$$U_L=0,\quad T_L=T_P \tag{10}$$

$$y\to\infty:\quad U_G=U_\infty,\quad T_G=T_\infty,\quad W=W_\infty \tag{11}$$

At the liquid-gas interface ($y=\delta(x)$), the matching conditions are :

(1) Continuity of velocity and temperature [17]:

$$U_{L,I}=U_{G,I}=U_I(x),\quad T_{L,I}=T_{G,I}=T_I(x) \tag{12}$$

(2) Continuity of shear stress :

$$\left(K\left|\frac{\partial U_L}{\partial y}\right|^{n-1}\frac{\partial U_L}{\partial y}\right)_I=\left(\mu_G\frac{\partial U_G}{\partial y}\right)_I=\tau_I(x) \tag{13}$$

(3) The transverse velocity component of the air-vapor mixture is deduced by assuming the liquid-gas interface to be semi-permeable (that is, the solubility of air into the liquid is negligibly small and the transverse velocity of air is zero at the interface) [18]:

$$V_{G,I}=-\left(\frac{D_V}{1-W_I}\frac{\partial W}{\partial y}\right)_I \tag{14}$$

(4) The mass fraction of vapor at the interface can be evaluated by [18] :

$$W_I=\frac{M_v P_I}{M_a(P-P_I)+M_v P_I} \tag{15}$$

Where P_I is the partial pressure of vapor at the gas-liquid interface.

(5) The interfacial vaporizing mass flux of vapor into the gas stream is :

$$\dot{m}_I=-\left(\frac{\rho_G D_V}{1-W_I}\frac{\partial W}{\partial y}\right)_I \tag{16}$$

(6) The heat balance at the interface implies :

$$\left(-\lambda_L \frac{\partial T_L}{\partial y}\right)_I = \left(-\lambda_G \frac{\partial T_G}{\partial y}\right)_I + (\dot{m}h)_I \quad (17)$$

This equation states that, at the interface, the heat is transferred from the liquid film into the gas stream by two modes. The first is the sensible heat due to the gas temperature gradient q_S, whereas the second is via the latent heat associated with the liquid film vaporization q_L. Thus the overall interfacial heat transfer from the liquid to the gas can be expressed as :

$$q_I = q_S + q_L \quad (18)$$

The conservation of the mass flow rate requires that, at any axial location, the following equation satisfied :

$$Q_0 = \int_0^{\delta(x)} \rho_L U_L dy + \int_0^x \dot{m}_I \, dx \quad (19)$$

Since the main concern is the evaporation of the liquid film, a dimensionless evaporation rate is introduced :

$$Mr = \frac{\int_0^x \dot{m}_I dx}{Q_0} \quad (20)$$

The dimensionless variables of the local liquid film thickness δ^*, the axial velocity U^*, the temperature T^* and the mass fraction of water vapor W^* are given by:

$$\delta^* = \frac{\delta}{L}\sqrt{\frac{U_\infty L}{\nu_{G,\infty}}} \quad (21)$$

$$U^* = \frac{U}{U_\infty} \quad (22)$$

$$T^* = \frac{T - T_\infty}{T_P - T_\infty} \quad (23)$$

$$W^* = \frac{W - W_\infty}{W_P - W_\infty} \quad (24)$$

W_P is the mass fraction of vapor defined at the plate temperature T_P.

SOLUTION METHOD

Since an analytical solution cannot be obtained for the coupled boundary-layer equations (2)-(8), the problem is solved by the finite difference numerical method. A fully implicit numerical scheme, in which the axial convection terms are approximated by the upstream difference and the transverse convection and diffusion terms by the central difference is marched downstream. The interface matching conditions for the shear stress and the heat flux are cast in backward difference for $(\partial\phi/\partial y)_G$ and in forward difference for $(\partial\phi/\partial y)_L$ where ϕ is U or T. Therefore, the governing equations in the liquid and gas flows can be solved simultaneously by the line-by-line method [19]. It is important to notice that the system of finite difference equations thus obtained result in a tridiagonal set which can be efficiently solved by the Thomas algorithm.

Since the thickness of the liquid film decreases with x due to the film evaporation, an homotopic transformation of the coordinates is employed to reduce the interface liquid-gas to a surface parallel to the plate. This avoids the need to rearrange the computational grid, thereby that one of the grid points is located at the liquid-gas interface. These homotopic coordinates are $X^* = x/L$ and $\eta = y/\delta$. In the flow direction, the grids are uniform ; in the transverse direction, they are uniform in the liquid phase and nonuniform in the gas-side.

RESULTS AND DISCUSSION

The influence of the humid air flow conditions, the inclination and temperature of the plate, and the liquid film inlet temperature on the evaporation of a falling Ostwaldian liquid film is analysed in terms of the evaporation rate and the liquid film thickness. Momentum, heat and mass transfer behavior is examined via the velocity, temperature and mass fraction distributions across the gas phase. Moreover, the one-dimensional, partial two-dimensional and two-dimensional approaches are compared to check the legitimacy of neglecting the inertia terms in the momentum equation for the liquid film.

Figure 2 shows the effects of the air flow conditions on the evaporation rate and the thickness of liquid film. As far as the free-stream velocity is concerned, it increases the thickness of both pseudoplastic and dilatant liquid films. A decrease in the air temperature or an increase in humidity causes a reduction of the film thickness.

The air temperature has no effect on the evaporation rate, a reduction in the air humidity results in higher evaporation rate. The effect of the free-stream velocity on the evaporation rate depends on the flow behaviour index. It is noted that, an increase in the velocity increases the evaporation rate as the flow behaviour index increases.

The influence of the inclination and the temperature of the plate on the film thickness and the evaporation rate is illustrated in Figure 3. As the inclination increases, the thickness decreases and the evaporation rate increases. A reduction of the plate temperature results in an increases of the thickness and a decrease of the evaporation rate.

The effect of the inlet temperature on the thickness and the evaporation rate is presented in Figure 4. It is noted that, the influence of the inlet temperature of the film increases as the flow index behaviour increases. A reduction of the inlet temperature causes an increase of the thickness and a decrease of the evaporation rate especially for dilatant liquids.

The variation of velocity, temperature and mass concentration distributions are shown in Figures 5 and 6. These are boundary-layer profiles, which depend on the flow behaviour index. The outer limit of the boundary-layer decreases as the flow behaviour index increases. Moreover, along the plate, the profiles increase and become linear.

Figure 7 includes a comparison between the thickness and the evaporation rate obtained in the one-dimensional, partial two-dimensional and two-dimensional approaches. It is clear, that the one-dimensional and the partial two-dimensional approaches are similar. However, the two-dimensional approach results in higher values for both the thickness and the evaporation rate. Also, the differences increase as the flow behaviour index increases. Thus, the inertia terms cannot be neglected because their contributions are of the same order of magnitude as those of the diffusion and gravity terms in the momentum equation of liquid film.

CONCLUSION

The evaporation of a falling Ostwaldian liquid film in a stream of humid air along an inclined flat plate is studied numerically. The governing equations with the interfacial matching conditions are solved numerically using a fully implicit finite-difference scheme. The influences of the air flow conditions, the plate inclination and temperature, as well as the inlet film temperature, on the evaporation rate and the liquid film thickness are presented. The velocity, temperature and the mass concentration through the

boundary-layer are also examined. A comparison between results obtained by the one-dimensional, partial two-dimensional and two-dimensional approaches is given. From the results, the following conlusions can be drawn :

(1) The air temperature has no effect on the evaporation rate or the thickness.
(2) An increase of the free-stream velocity increases the thickness and the evaporation rate except in the case where $n = 0.7$.
(3) A reduction in the air humidity increases the evaporation rate and decreases the thickness.
(4) Higher evaporation rate and lower thickness are experienced with higher plate temperature and inclination.
(5) Lower inlet temperature of the film causes lower evaporation rate and higher thickness especially for dilatant liquids.
(6) The inertia terms cannot be neglected in the momentum equation for the liquid film compared to the diffusion of the gravity terms.

REFERENCES

[1] Chow LC and Chung JN. Evaporation of water into a laminar stream of air and superheated steam. Int. J. Heat Mass Transfer 1983; 26 (3): 373-380.

[2] Shembharkar TR and Pai BR. Prediction of film cooling with a liquid coolant. Int. J. Heat Mass Transfer 1986; 29 (6): 899-908.

[3] Suzuki K , Hagiwara Y and Sato S. Heat transfer and flow characteristics of two-phase two-component annular flow. Int. J. Heat Mass Transfer 1983; 26 (4): 597-605.

[4] Yan WM and Lin TF. Combined heat and mass transfer in natural convection between parallel plates with film evaporation. Int. J. Heat Mass Transfer 1990; 33 (3): 529-541.

[5] Tsay YL, Lin TF and Yan WM. Cooling of falling liquid film through interfacial heat and mass transfer. Int. J. Mutiphase flow 1990; 16: 853-865 (1990).

[6] Baumann WW and Thiele F. Heat and mass transfer in evaporating two-component liquid film flow. Int. J. Heat Mass Transfer 1990; 33 (2): 267-273.

[7] Mammou M and Daguenet M. Numerical study of heat and mass transfer from inclined flat plate with wet and dry zones. Int. J. Heat Mass Transfer 1992; 35 (9): 2277-2287.

[8] Yan WM. Turbulent mixed convection heat and mass transfer in wetted channel, J. Heat Transfer 1995; 117 (1): 229-233.

[9] Agunaoun A, Daif A, Barriol R et Daguenet M. Évaporation en convection forcée d'un film mince s'écoulant en régime permanent, laminaire et sans ondes, sur une surface plane inclinée. Int. J. Heat Mass Transfer 1994; 37 (18): 2947-2956.

[10] Agunaoun A, Kaoua M, Daïf A et Daguenet M. Évaporation en convection mixte d'un film mince s'écoulant sur une surface plane inclinée. Rev. Gén. Therm. 1996 ; 35 (414): 373-385.

[11] Yan WM and Soong CY. Convective heat and mass transfer along an inclined heated plate with film evaporation. Int. J. Heat Mass Transfer 1995; 38 (7): 1261-1269.

[12] He S, An P, Li J and Jackson JD. Combined heat and mass transfer in a uniformly heated vertical tube with water film cooling. Int. J. Heat and Fluid Flow 1998; 19 (5): 401-417.

[13] Feddaoui M, Belahmidi E, Mir A and Bendou A. Numerical study of evaporative cooling of liquid film in laminar mixed convection tube flows. Int. J. Therm. Sci 2001; 40 (11): 1011-1020.

[14] Mezaache E and Daguenet M. Étude numérique de l'influence de l'inclinaison sur l'évaporation d'un film liquide s'écoulant sur une paroi plane isotherme ou à flux de chaleur imposé Can. J. Chem. Eng. 1998; 76 :203-210.

[15] Mezaache E and Daguenet M. Étude numérique de l'évaporation dans un courant d'air humide d'un film d'eau ruisselant sur une plaque inclinée. Int. J. Therm. Sc 2000 ; 39 (1), 117-129.

[16] Benkhaled A, Saouli S, M'Bow C and Daguenet M. Étude numérique du transfert de chaleur entre l'air et un film mince ostwaldien en régime laminaire permanent sur une surface plane inclinée isotherme. Int. J. Therm. Sc ; 42 (4) to be published.

[17] Delhaye J.M. Conditions d'interface et sources d'entropie dans les systèmes diphasiques. Rapport CEA-R-4562, 1974.

[18] Eckert ERG and Drake RM. Analysis of heat and mass transfer. New York : McGraw-Hill., 1972.

[19] Patankar SV. Numerical heat transfer and fluid flow. New York : McGraw-Hill., 1980

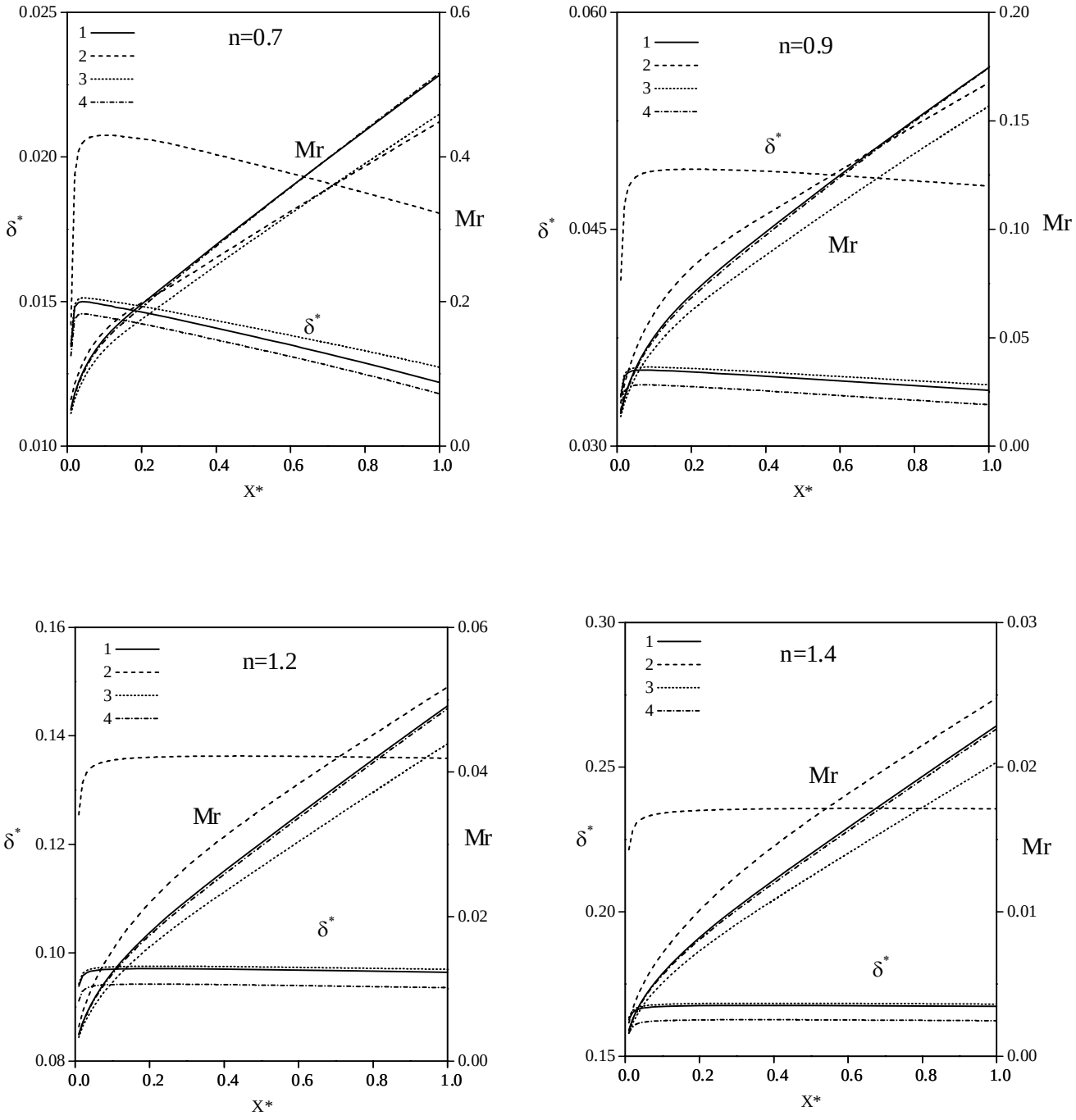

Figure 2: Influence of the air flow conditions on the film thickness δ^* and the evaporation rate Mr .

$T_P = T_{L0} = 50\,°\text{C}, \theta = 10\,°$

1 : $U_\infty = 1\,\text{m/ s}\,, W_\infty = 0{,}001\,, T_\infty = 20\,°\text{C}$, **2** : $U_\infty = 2\,\text{m/ s}\,, W_\infty = 0{,}001\,, T_\infty = 20\,°\text{C}$

3 : $U_\infty = 1\,\text{m/ s}\,, W_\infty = 0{,}01\,, T_\infty = 20\,°\text{C}$, **4** : $U_\infty = 1\,\text{m/ s}\,, W_\infty = 0{,}001\,, T_\infty = 30\,°\text{C}$

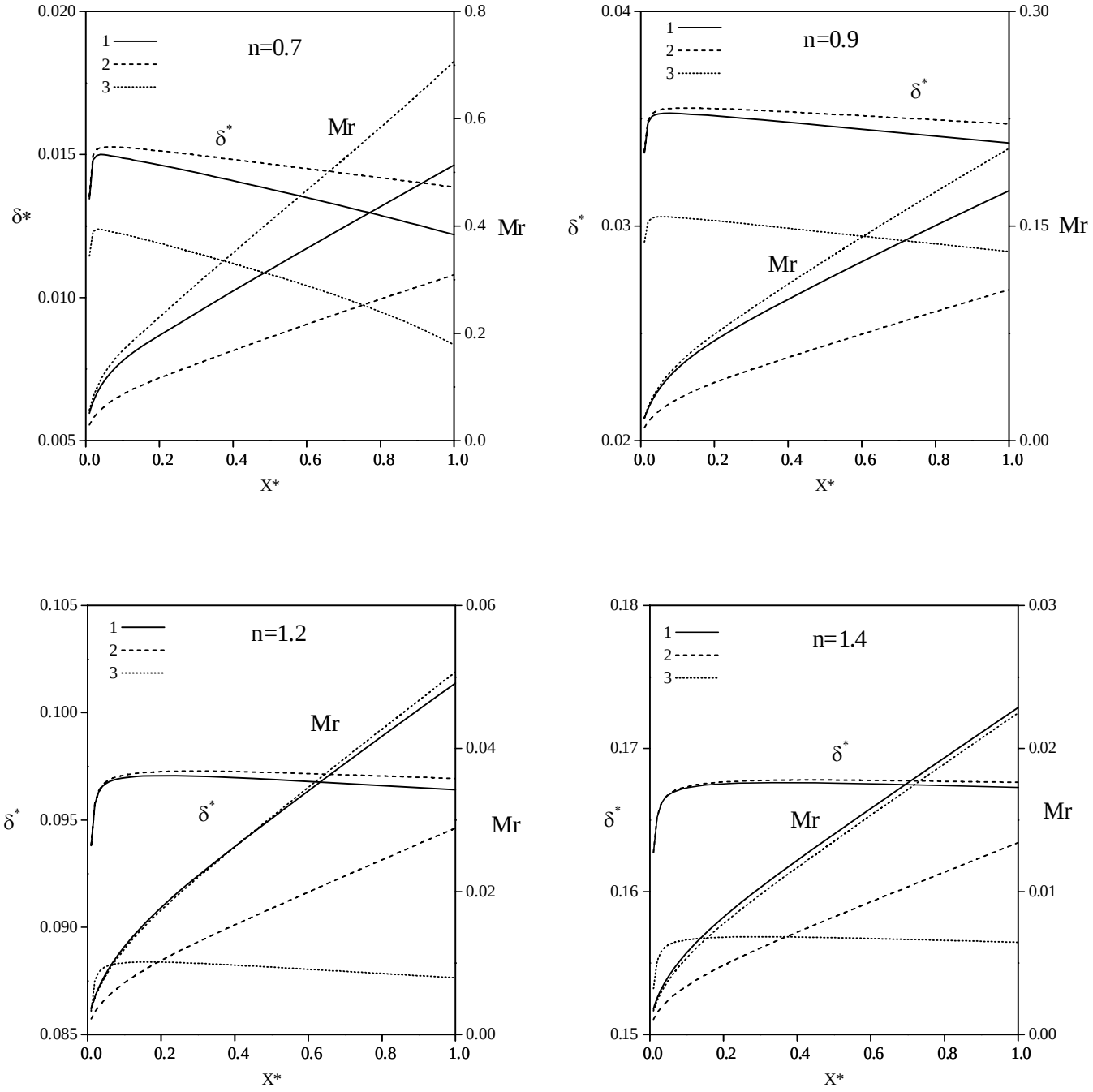

Figure 3: Influence of the inclinaison and the temperature of the plate on the film thickness δ^* and the evaporation rate Mr .
$U_\infty = 1\,\text{m/ s}, W_\infty = 0{,}001, T_\infty = 20\,°\text{C}$
1 : $T_p = 50\,°\text{C}, \theta = 10\,°$, **2** : $\text{Tp} = 40\,°\text{C}, \theta = 10\,°$, **3** : $T_p = 50\,°\text{C}, \theta = 15\,°$

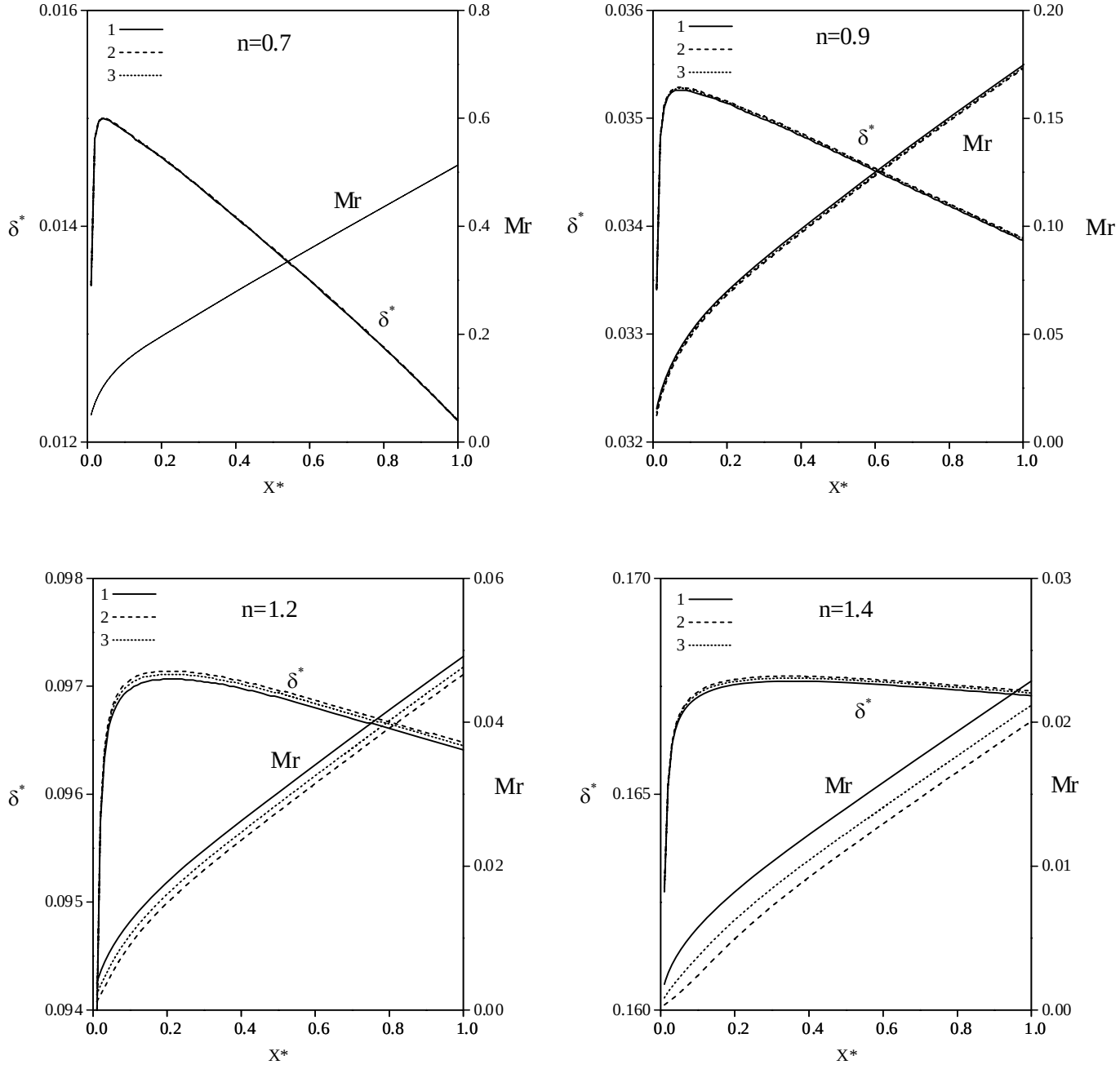

Figure 4: Influence of the inlet temperature of the liquid film on the film thickness δ^* and the evaporation rate Mr .
$U_\infty = 1\,\mathrm{m/s}, W_\infty = 0{,}001, T_\infty = 20\,°\mathrm{C}, T_P = 50\,°\mathrm{C}, \theta = 10\,°$
1 : $T_{L0} = 50\,°\mathrm{C}$, **2** : $T_L = 20\,°\mathrm{C}$, **3** : $T_{L0} = 35\,°\mathrm{C}$

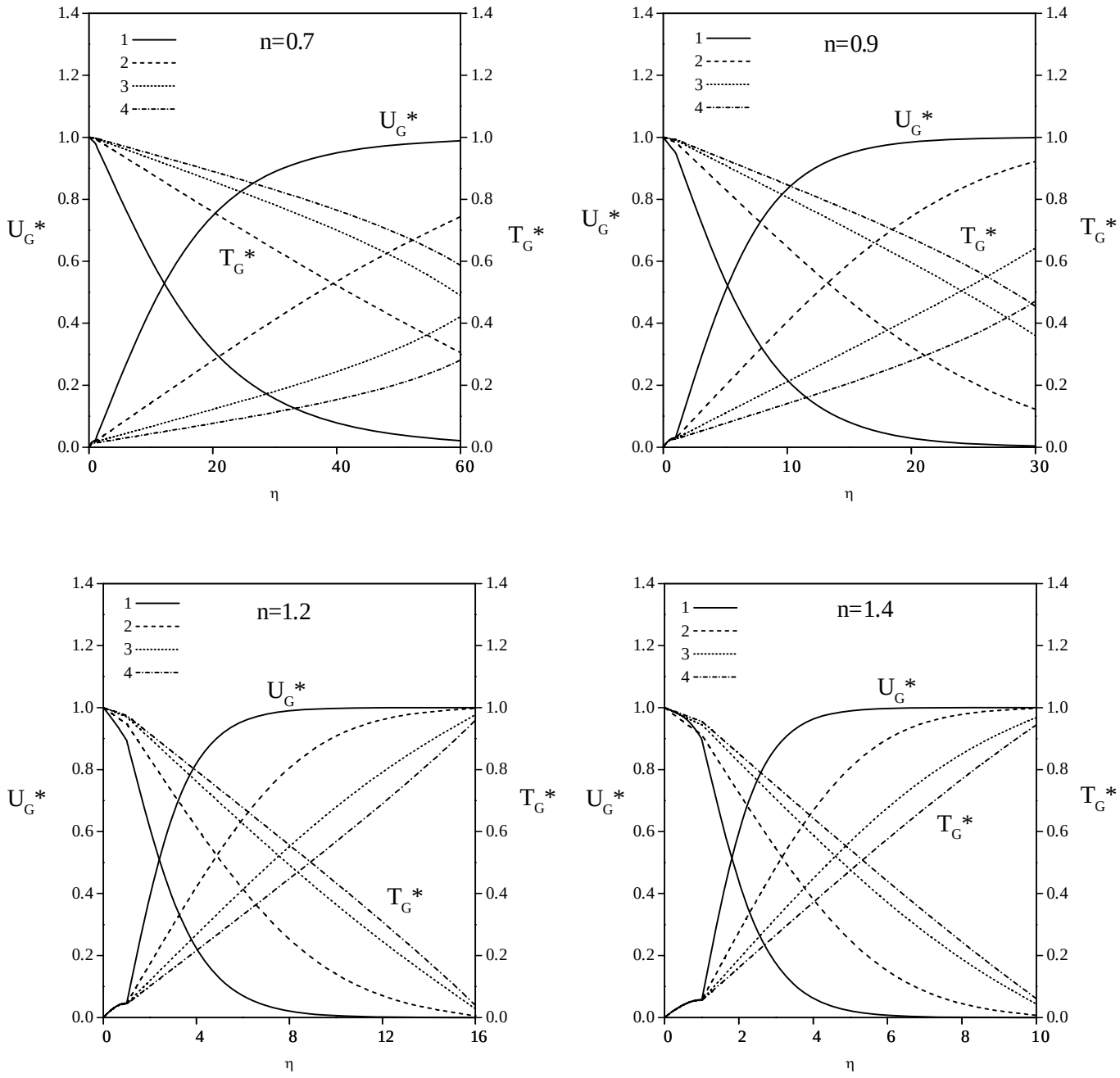

Figure 5: Development of the velocity and temperature profiles.
$T_P = T_{L0} = 50\,°\text{C}, U_\infty = 1\ \text{m.s}^{-1}, W_\infty = 0{,}001\ , T_\infty = 20\,°\text{C}, \theta = 10\,°\text{C}$
1 : $X^* = 0{,}02$, **2** : $X^* = 0{,}10$, **3** : $X^* = 0{,}30$, 4 : $X^* = 0{,}90$

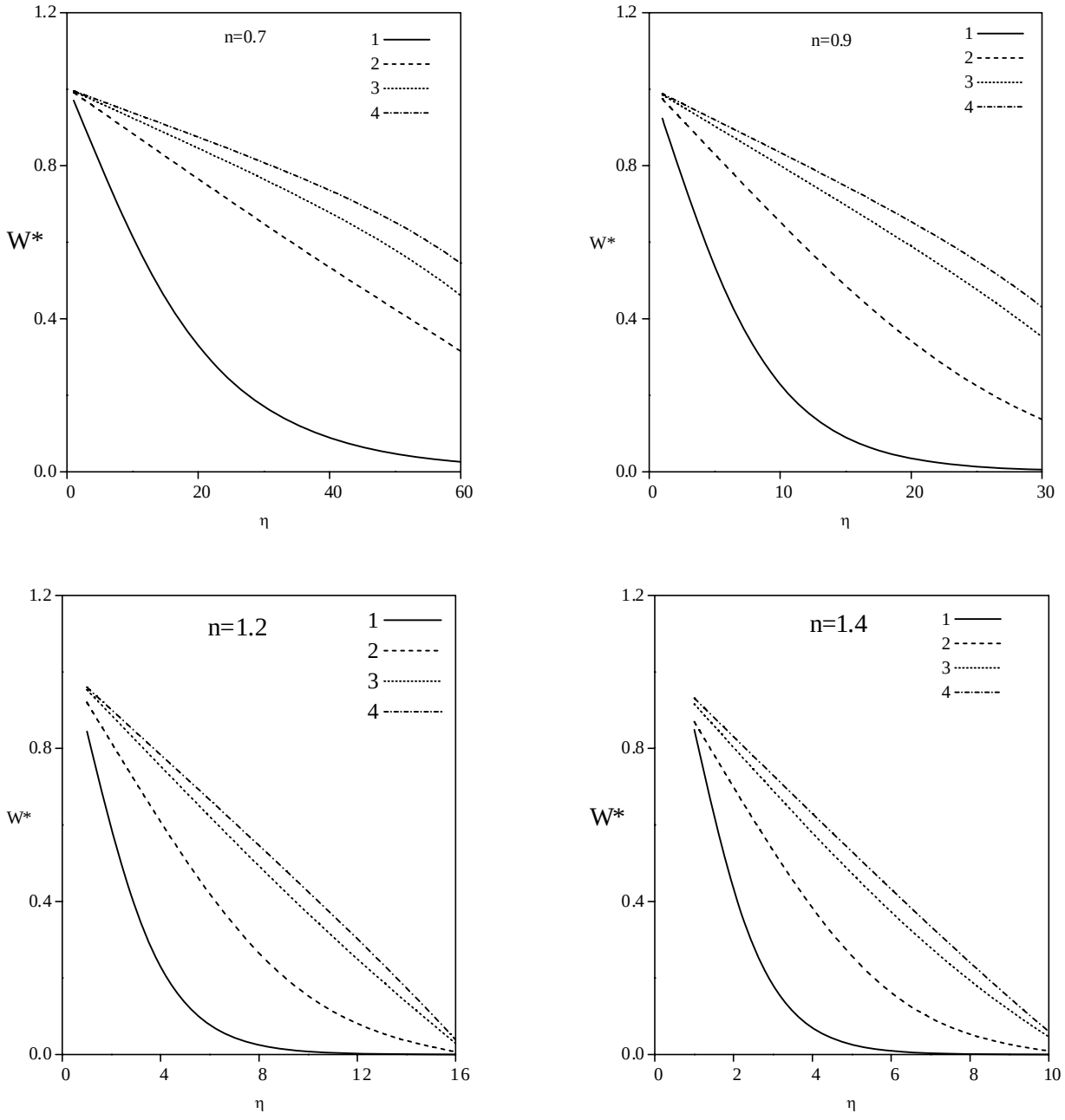

Figure 6: Development of the mass concentration profiles.
$T_P = T_{L0} = 50\,°\text{C}, U_\infty = 1$ m/ s, $W_\infty = 0{,}001$, $T_\infty = 20\,°\text{C}, \theta = 10\,°\text{C}$
1 : $X^* = 0{,}02$, **2** : $X^* = 0{,}10$, **3** : $X^* = 0{,}30$, 4 : $X^* = 0{,}90$

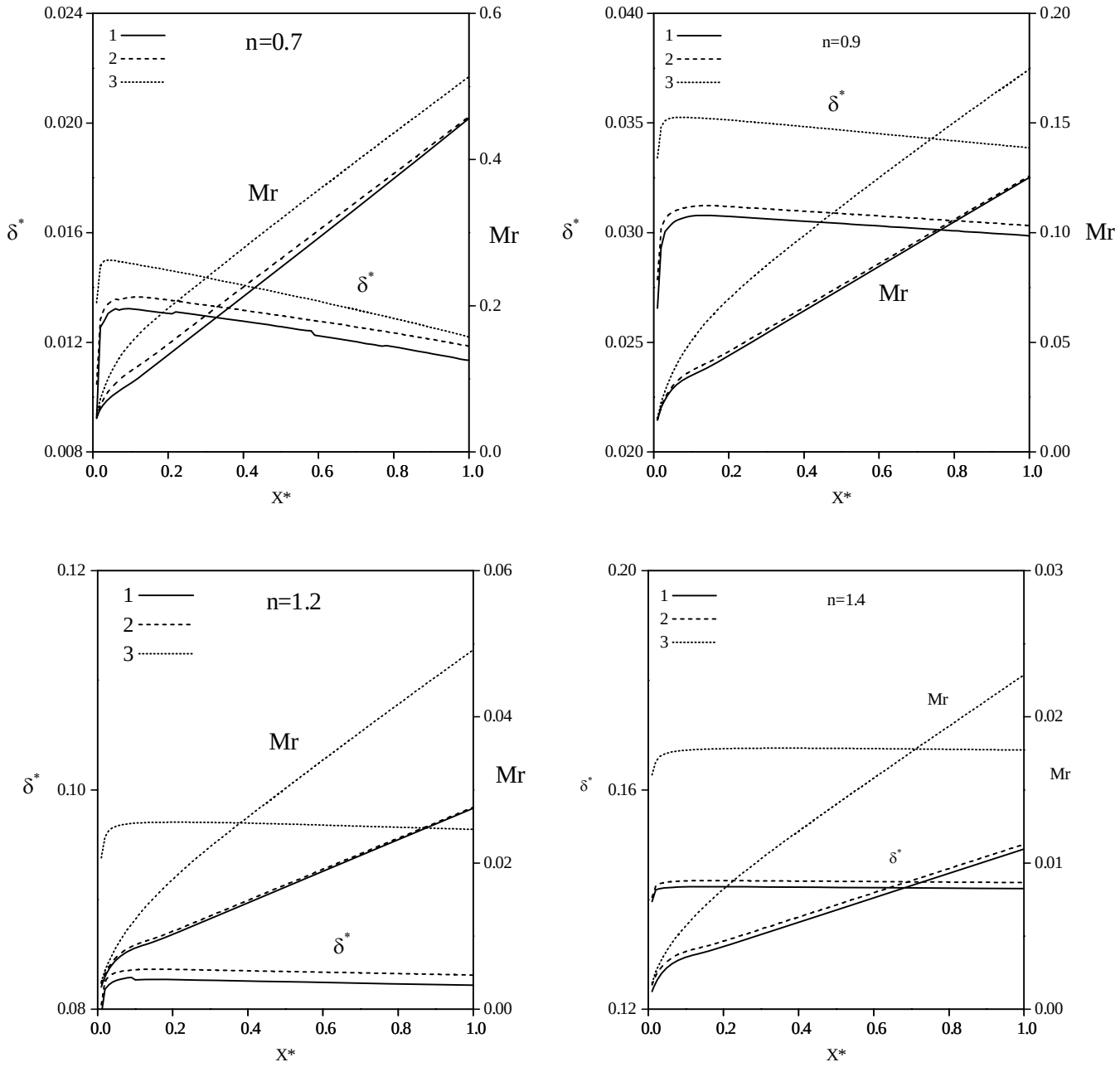

Figure 7: Influence of the inertia terms on the film thickness δ^* and the evaporation rate Mr .
$T_P = T_{L0} = 50\,°C, U_\infty = 1$ m/ s, $W_\infty = 0{,}001$, $T_\infty = 20\,°C, \theta = 10\,°C$
1 : one-dimensional approach, **2** : partial two-dimensional approach, **3** : two-dimensional approach.